Editors' Suggestion | Featured in Physics

Direct Measurement of Capillary Attraction between Floating Disks

Ian Ho,[1] Giuseppe Pucci,[1,2] and Daniel M. Harris[1,*]
[1]School of Engineering, Brown University, 184 Hope Street, Providence, Rhode Island 02912, USA
[2]Univ Rennes, CNRS, IPR (Institut de Physique de Rennes)—UMR 6251, F-35000 Rennes, France

(Received 10 June 2019; revised manuscript received 3 September 2019; published 19 December 2019)

Two bodies resting at a fluid interface may interact laterally due to the surface deformations they induce. Here we use an applied magnetic force to perform direct measurements of the capillary attraction force between centimetric disks floating at an air-water interface. We compare our measurements to numerical simulations that take into account the disk's vertical displacement and spontaneous tilt, showing that both effects are necessary to describe the attraction force for short distances. We characterize the dependence of the attraction force on the disk mass, diameter, and relative spacing, and develop a scaling law that captures the observed dependence of the capillary force on the experimental parameters.

DOI: 10.1103/PhysRevLett.123.254502

Capillary attraction between floating bodies has been a subject of curiosity and scientific interest for over 70 years within physics and engineering, although qualitative descriptions of the phenomenon extend even further back in the history of science. One of the first mathematical explorations of capillary attraction was by Nicolson, who demonstrated that the attraction between bubbles at a free surface was due to the presence of buoyancy-induced interfacial deformation [1]. This early modeling work was inspired by the experimental observations of Bragg, who used self-assembled aggregates of monodisperse bubbles as an analog system for atomic crystal physics [2,3]. Since that time, it is now well understood that two bodies resting at a fluid interface may attract through their mutual surface deformation in order to minimize the gravitational and surface energy of the system [4]. Furthermore, interesting analogies have also recently been established between capillary attraction and electrostatic repulsion due to the similarity of the governing equations in certain regimes [5–8]. Capillary interactions have been a topic of focus in several review articles [8–11]. Recently, this effect has been popularized and called the "Cheerios effect" [12], after the casual observation that the famous breakfast cereal tends to cluster on milk rather than remaining dispersed at the interface.

This aggregation mechanism has seen a resurgence of interest beyond pure curiosity, as the effect has recently been harnessed for numerous applications involving particle self-assembly at fluid interfaces [10,13,14] and to rationalize a number of observations in natural systems [15–20]. Despite significant efforts to theoretically rationalize the capillary interaction between floating bodies [1,4–7,12,21–30], direct measurements of this force are relatively limited.

Some direct measurements of capillary attraction forces have been performed on bodies that are rigidly fixed to a force sensing apparatus rather than on floating bodies [31–36]. In other works, the attraction force of floating bodies has been *indirectly* extracted through measurement of the velocity as two particles freely move toward one another (for example, see Refs. [12,37]). The rate of change of the velocity of approach can then be related to the net hydrodynamic force. However, in order to isolate the component due to mutual attraction, a drag law must also be included in this computation, which is often complicated due to the potentially subtle contact line dynamics [24] and the mutual flow-induced interactions as the particles approach [38]. Ultimately, only a few *direct* measurements of the capillary attraction force between floating bodies have been reported. Recently, several groups have used optical micromanipulation to perform direct measurements of the capillary forces between microscopic colloidal particles at a fluid interface [39–41]. At the macroscopic scale, some earlier work by Mansfield *et al.* measured the "binding" force between two floating centimetric plates in contact by gradually applying a known horizontal force via a flexible thread and a torsion balance until the plates separated [42]. However, very few parameters were explored in their investigation and the force as a function of plate spacing was not explored.

In this Letter, we report direct measurements of the capillary attraction force between pairs of floating macroscopic disks on an air-water interface using a novel experimental setup, directly compare our results to numerical simulations, and rationalize the dependence of the capillary attraction force on the disk mass, radius, and relative spacing.

The experimental configuration is shown in Fig. 1. Two cylindrical disks with identical radius R and mass m were placed on the surface of a water bath with density ρ and surface tension σ. The water interface beneath the disk is deformed by a mean displacement δ, which results from the

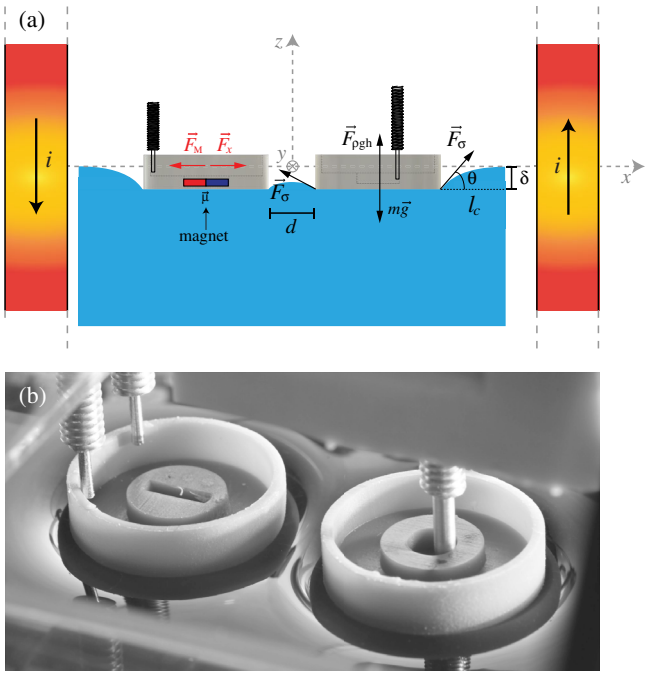

FIG. 1. (a) Schematics of the experimental setup for direct measurements of the attraction force between floating disks. Relevant forces which lead to vertical equilibrium (floating) are highlighted on the disk on the right. The capillary attraction force $\vec{F}_x$, which is balanced by the imposed magnetic force $\vec{F}_M$, is depicted on the disk on the left. (b) Photograph of two disks in the experimental apparatus as they deform the free surface and attract one another. See the video in Supplemental Material for a typical experimental run [46].

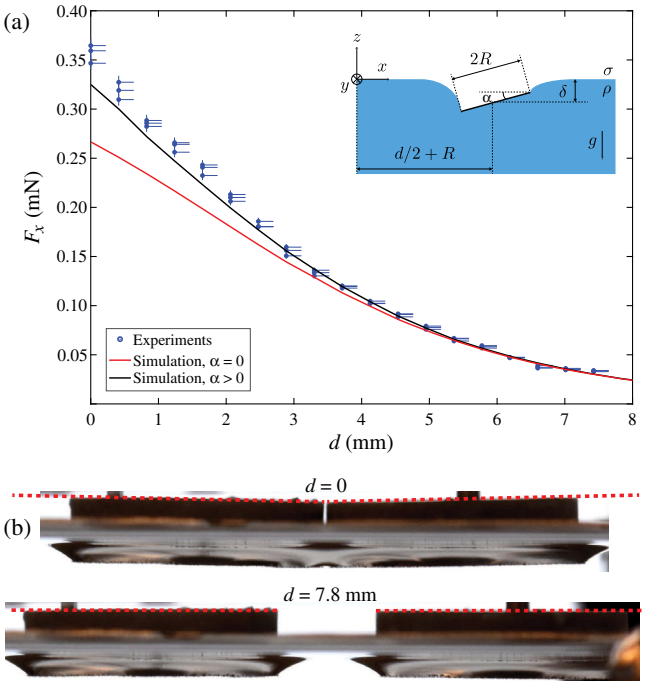

FIG. 2. (a) Capillary attraction force F_x vs distance d between disks as measured in experiments and compared to numerical simulations. Disks have radius $R = 1.0$ cm and mass $m = 0.90$ g. Inset: Schematic of the geometrical configuration considered in the numerical simulations. (b) Side view of disks at $d = 0$ (top) and $d = 0.78$ cm (bottom) demonstrating presence of inward tilt for $d = 0$. $\alpha = 1.22°$ inward tilt is numerically predicted for $d = 0$, as indicated by the red dashed line.

equilibrium of the body's weight $m\vec{g}$, hydrostatic force $\vec{F}_{\rho gh}$, and capillary force $\vec{F}_\sigma$ [Fig. 1(a)] [43,44]. The disks were 3D printed and made to be superhydrophobic using a commercially available spray coating to increase the advancing contact angle and thus ensure that the interface remained pinned to the bottom perimeter of each disk. One disk was initially held laterally in place by two rods that were in contact with its inner vertical surface in order to balance the capillary attraction force due to the neighboring disk. A third rod was in contact with the second disk's inner vertical surface. This rod was mounted to a linear translation stage driven by a stepper motor, which allowed for automated control of the distance d between the disks. The first disk was embedded with a permanent magnet with magnetic moment $\vec{\mu}$ aligned along the coil axis. The bath was surrounded by two coils with current i flowing in opposite directions, which generated a constant magnetic field gradient $\partial_x B_x(i) = \beta i$ along the coil axis [45]. The permanent magnet was positioned at the geometric center of the two-coil configuration and thus experienced a force $F_M = -\mu\beta i$, where $\mu = |\vec{\mu}|$. At the beginning of each measurement, we started with the disks in contact with one another and we progressively moved the rod (by steps of $\Delta d = 0.2$ mm) until a visible gap could be seen between the disks. We defined this position as the disk spacing of $d = 0$. The disk spacing d was then increased by moving the right disk a prescribed distance using the automated translation stage. At each spacing, we gradually increased the current i in the coils. When the magnetic force exceeded the capillary force, the disk with the embedded magnet (shown as the left-hand disk in Fig. 1) drifted away from its partner and the current value was recorded. We repeated the procedure by increasing the distance d between the disks up to approximately 1 cm. For a pair of disks with masses m and radii R, the critical value of current $i_d(d)$ to achieve disk separation was computed by averaging the results from three disk pairs, on each of which three independent measurements were performed. The capillary force as a function of distance was then given by $F_x(d) = -F_M(d) = \mu\beta i_d(d)$. We emphasize that the critical value of the current is recorded at the moment of separation, at which the normal force on the disks from the vertical rods vanishes. Thus the measurements are not influenced by physical contact with the measurement apparatus. Extended details of the experimental setup and protocol can be found in Supplemental Material [46].

In Fig. 2(a) we present a sample experimental dataset of the capillary attraction force F_x vs the distance d between the disks. The force decreases monotonically with the

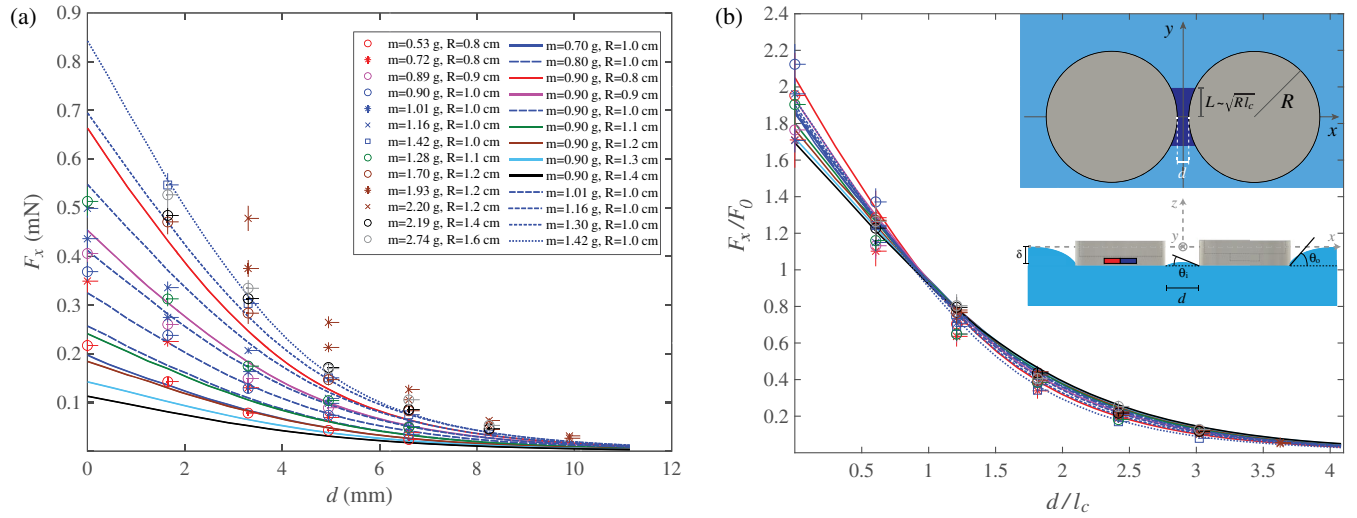

FIG. 3. Ensemble of experimental (points) and numerical (lines) data for pairs of disks with different mass m and radius R. (a) Dimensional capillary force F_x vs distance d between disks. (b) Dimensionless capillary force F_x/F_0 vs dimensionless distance between the disks d/l_c. F_0 is defined in Eq. (13).

spacing, as it is expected since the anomalous surface displacement due to the neighboring disk decays as the disks separate. Experimental data are compared to numerical simulations that solve the Young-Laplace equation for the free surface shape using the disk perimeter as a boundary condition. The disks were modeled as plates with radius R, mass m, and infinitesimal thickness. In the first set of simulations we fixed the disks so that no rotation around the y axis was included (thus the disk remained strictly parallel to the undisturbed free surface). We computed the force and found that it adequately captures the experimental force for large separation distances, but was somewhat unsatisfactory in the short range. We thus extended the numerical simulations by allowing for tilt around the y axis (directly toward or away from the neighboring disk), thus including both the balance of moments and forces on the disk. For each combination of m, R, and d, the surface deformation δ and the tilt angle α were determined uniquely by identifying the pair of values (δ, α) for which the disks were in vertical equilibrium as prescribed by

$$F_z = F_{\sigma,z} + F_{g,z} = mg, \tag{1}$$

and rotational equilibrium as prescribed by

$$M_y = M_{\sigma,y} + M_{g,y} = 0, \tag{2}$$

where F_σ, M_σ and F_g, M_g are forces and moments due to surface tension and hydrostatic forces, respectively. Typical values are $\delta \lesssim 0.2$ cm and $\alpha \lesssim 2°$, and the magnitude of both δ and α decreases as the disks are separated. Once δ and α were determined, the horizontal attractive force was computed by summing the lateral contributions from surface tension and hydrostatic pressure,

$$F_x = -(F_{\sigma,x} + F_{g,x}), \tag{3}$$

where the overall minus sign is chosen to have $F_x > 0$ for attraction. The attraction force corresponding to Eq. (3) better captures the experimental behavior for both long and short separation distances [Fig. 2(a)] with no fitting parameters. We also present side view images of the disks in Fig. 2(b), which experimentally confirm the presence of an inward tilt for small disk spacings. We suspect that the relatively small remaining discrepancy at small spacings may be due to our lone approximation of the disks being of negligible thickness. Despite the fact that the emergent tilt angle is rather small, our model demonstrates that its inclusion is necessary to adequately describe the capillary attraction in the short range. Extended details on the numerical simulations can be found in Supplemental Material [46].

We proceeded by exploring the dependence of the capillary force on the disk mass m and radius R. In experiments, we first fixed the radius $R = 1.0$ cm and varied the mass from $m = 0.70$ to 1.42 g. We observe that the capillary force F_x monotonically increases with mass, as expected for heavier bodies that induce larger surface deformations. Experimental data and trends are similarly well captured by numerical simulations. We then explored the dependence of the attraction force on the disk radius by fixing the mass at $m = 0.90$ g and varying the radius from $R = 0.8$ to 1.4 cm in the numerical simulations. We find that the capillary force decreases with the disk radius, a consequence of the larger contact area and perimeter, which result in smaller overall surface deformation.

The ensemble of experimental and numerical data collected are presented in Fig. 3(a), in which the magnitude of the force depends on both the mass and the radius of the disks. In an attempt to isolate these dependencies, we develop a scaling analysis for the typical magnitude of the

attraction force. Dimensional analysis suggests that the attraction force could be described by the following dimensionless law:

$$\frac{F_x}{F_0} = f\left(\frac{d}{l_c}, \frac{\delta}{l_c}, \frac{R}{l_c}\right), \tag{4}$$

where f is an unknown function and F_0 is a typical force scale that must depend on the mass m. The relevant length scale chosen is the capillary length, $l_c = \sqrt{\sigma/\rho g}$, which represents the distance over which hydrostatic pressure balances curvature pressure due to surface tension (e.g., the characteristic length of a fluid meniscus) [47]. For clean water at room temperature, $l_c = 2.7$ mm. To facilitate the scaling analysis, we assume small deformations $\delta \ll l_c$, large disk size $R \gg l_c$, and that the disks are close to each other $d \ll l_c$. The net horizontal capillary force per unit length acting on a disk scales as

$$\frac{F_{\sigma,0}}{L} \sim \sigma(-\cos\theta_i + \cos\theta_o), \tag{5}$$

where θ_i is the angle formed by the water free surface and the disk in between the pair (along the x axis), and θ_o is the angle that water forms with the far portion of the disk (along the x axis). L is the characteristic length scale in y of the interaction region over which the free surface is disturbed from its axisymmetric profile in isolation. For a single disk in isolation centered at $r = 0$, the meniscus takes the form of an outwardly decaying exponential, $u(r) = -\delta e^{-(r-R)/l_c}$ for $r \geq R$, which is valid under our assumptions $\delta \ll l_c$ and $R \gg l_c$ [47]. From this expression, it can be readily shown that the contact angle in equilibrium is given by

$$\theta = \delta/l_c \tag{6}$$

to leading order. We further assume that $R \gg L$, so that outside of the interaction region $\theta_o \approx \theta$, an assumption we will revisit later. For disks that are nearly in contact ($d \ll l_c$) we can also assume that $\theta_i \ll \theta_o$, as the slope of the interface in between the disks is much smaller than that of the outer deformation. This assumption is physically justified by the fact that the contact line is pinned at the bottom edges of the disks; thus when the identical disks are in very close proximity to one another, the fluid interface spanning them is approximately flat.

The extent of the interaction region L along the y axis can be estimated by expanding the disk equation in the plane $x = -\sqrt{R^2 - y^2} + R + d/2$ for $y/R \ll 1$ and recalling that $d/R \ll 1$ (since we have assumed $d/l_c \ll 1$ and $R/l_c \gg 1$). To leading order we thus obtain $x/R \approx (y/R)^2/2$. As the extent of the interaction occurs up to a lateral separation $x \sim l_c$, we obtain

$$L \sim \sqrt{Rl_c} \tag{7}$$

as the typical interaction length along the y direction. Using the result derived in Eq. (7), it can be seen that the condition $R \gg L$ is consistent with $R \gg l_c$, as initially assumed.

Substituting our results into Eq. (5) and expanding the cosine terms, we find that the capillary attraction scales as

$$F_{\sigma,0} \sim \sigma\frac{\delta^2 R^{1/2}}{l_c^{3/2}}. \tag{8}$$

This result is consistent with recent rigorous asymptotic approaches to the problem under the same assumptions [30]. However, in order to complete our scaling analysis we must finally estimate how δ scales with the other parameters. For a single disk in isolation the vertical force balance required for flotation yields

$$mg = \pi R^2 \rho g \delta + 2\pi R\sigma \sin\theta. \tag{9}$$

Upon substituting Eq. (6) into Eq. (9), we find

$$\delta = \frac{mg}{\pi\sigma[(R/l_c)^2 + 2R/l_c]}. \tag{10}$$

Note that $(R/l_c)^2 = \rho g R^2/\sigma = \mathrm{Bo}$, often referred to as the Bond number, which represents the relative influence of gravity and surface tension in the vertical direction.

The hydrostatic contribution to the attractive force (due to the spontaneous inward tilt angle α) is $F_{g,0} = \rho g \delta R^2 \sin\alpha$. In order to estimate α, we consider the equilibrium of moments $M_{g,y} \sim M_{\sigma,y}$. Scaling of this equation yields $\rho g R^4 \sin\alpha \sim \sigma\delta R^{3/2} l_c^{-1/2}$ and, thus, $\sin\alpha \sim l_c^{3/2}\delta R^{-5/2}$. We finally obtain

$$F_{g,0} \sim \sigma\delta^2/\sqrt{Rl_c}. \tag{11}$$

We thus have

$$\frac{F_{g,0}}{F_{\sigma,0}} \sim \frac{l_c}{R}, \tag{12}$$

where we see that under our assumption $R \gg l_c$ the hydrostatic component of the attractive force is small relative to the contribution from surface tension. We thus take our characteristic attractive force F_0 as the contribution from capillarity alone in Eq. (8) with δ from Eq. (10):

$$F_0 = \frac{(mg)^2 R^{1/2}}{\pi^2\sigma l_c^{3/2}[(R/l_c)^2 + 2R/l_c]^2}. \tag{13}$$

Considering the explicit relationship between F_0, δ, and R through Eqs. (10) and (13), under our assumptions, the nondimensional law in Eq. (4) reduces to

$$\frac{F_x}{F_0} = f\left(\frac{d}{l_c}\right). \tag{14}$$

We normalize the force data by F_0 and the spacing by l_c and we show that our results nearly collapse onto a single curve [Fig. 3(b)]. This collapse is somewhat surprising given that the vertical displacements δ are frequently large in both our experiments and simulations, often on the same order as the capillary length. However, in the derivation of the scaling analysis, the condition $\delta \ll l_c$ is used only to derive Eq. (6). Numerical solution of the axisymmetric Young-Laplace equation for an isolated disk indicates that $\theta = \delta/l_c$ does in fact remain a decent approximation for $\delta \sim l_c$ when $R \gg l_c$. The collapse suggests that we have satisfactorily captured the leading order effects in the problem. A more rigorous asymptotic approach may be able to identify the next order corrections and further rationalize the remaining spread in our data.

In this work, we performed *direct* measurements of the capillary attraction between *macroscopic* bodies resting at an air-water interface. Specifically, we measured the attraction force between two centimetric disks as a function of their radius, mass, and relative spacing. We complemented the experimental study with numerical simulations that compare well to the experimental data. We isolated the role of the spontaneous inward tilt of the disks, which was found to be necessary to quantitatively describe the attraction force in the short range. In addition, we developed a scaling law for the capillary attraction force as a function of the distance between the disks and achieved a satisfactory collapse of our data over a range of disk masses and radii. We expect our results to be directly relevant to a number of natural and artificial systems, including living organisms [48] and bioinspired microrobots [49–51] moving at the air-water interface.

Measurements have been performed by means of a custom experimental setup based on a controllable magnetic applied force. In contrast to prior work where magnetic forcing has been used to complement fluid-solid interactions [52–54], here we use the magnetic force as a tool to measure fluid forces without physical contact. Our measurement platform could be readily adapted to quantitatively explore more exotic effects such as the interaction of anisotropic objects [55–57], objects on curved interfaces [27,58–61], elastic structures [62], interactions of particles and capillary waves [63–65], dynamic interactions of particles [66–68], or even potentially the "inverted Cheerios effect" [69].

D. M. H. would like to thank the Brown OVPR Seed Award for partial support of this work. Additionally, G. P. thanks the CNRS Momentum program for its support.

*daniel_harris3@brown.edu

[1] M. Nicolson, Math. Proc. Cambridge Philos. Soc. **45**, 288 (1949).
[2] L. Bragg, J. Sci. Instrum. **19**, 148 (1942).
[3] W. L. Bragg and J. Nye, Proc. R. Soc. A **190**, 474 (1947).
[4] W. Gifford and L. Scriven, Chem. Eng. Sci. **26**, 287 (1971).
[5] M. M. Müller, M. Deserno, and J. Guven, Europhys. Lett. **69**, 482 (2005).
[6] J.-B. Fournier, Soft Matter **3**, 883 (2007).
[7] A. Domínguez, M. Oettel, and S. Dietrich, J. Chem. Phys. **128**, 114904 (2008).
[8] A. Domínguez, in *Structure and Functional Properties of Colloidal Systems*, edited by R. Hidalgo-Alvarez (CRC Press, Boca Raton, 2009), pp. 31–59.
[9] P. A. Kralchevsky and K. Nagayama, Adv. Colloid Interface Sci. **85**, 145 (2000).
[10] I. B. Liu, N. Sharifi-Mood, and K. J. Stebe, Annu. Rev. Condens. Matter Phys. **9**, 283 (2018).
[11] J. Liu and S. Li, Eur. Phys. J. E **42**, 1 (2019).
[12] D. Vella and L. Mahadevan, Am. J. Phys. **73**, 817 (2005).
[13] N. Bowden, A. Terfort, J. Carbeck, and G. M. Whitesides, Science **276**, 233 (1997).
[14] N. Aubry, P. Singh, M. Janjua, and S. Nudurupati, Proc. Natl. Acad. Sci. U.S.A. **105**, 3711 (2008).
[15] D. L. Hu and J. W. Bush, Nature (London) **437**, 733 (2005).
[16] J. W. Bush, D. L. Hu, and M. Prakash, Adv. Insect Physiol. **34**, 117 (2007).
[17] N. J. Mlot, C. A. Tovey, and D. L. Hu, Proc. Natl. Acad. Sci. U.S.A. **108**, 7669 (2011).
[18] J. Loudet and B. Pouligny, Eur. Phys. J. E **34**, 76 (2011).
[19] J. Voise, M. Schindler, J. Casas, and E. Raphaël, J. R. Soc. Interface **8**, 1357 (2011).
[20] P. Peruzzo, A. Defina, H. M. Nepf, and R. Stocker, Phys. Rev. Lett. **111**, 164501 (2013).
[21] D. Chan, J. Henry, Jr., and L. White, J. Colloid Interface Sci. **79**, 410 (1981).
[22] P. Kralchevsky, V. Paunov, I. Ivanov, and K. Nagayama, J. Colloid Interface Sci. **151**, 79 (1992).
[23] B. A. Grzybowski, N. Bowden, F. Arias, H. Yang, and G. M. Whitesides, J. Phys. Chem. B **105**, 404 (2001).
[24] P. Singh and D. Joseph, J. Fluid Mech. **530**, 31 (2005).
[25] K. D. Danov and P. A. Kralchevsky, Adv. Colloid Interface Sci. **154**, 91 (2010).
[26] H. N. Dixit and G. Homsy, Phys. Fluids **24**, 122102 (2012).
[27] M. Cavallaro, L. Botto, E. P. Lewandowski, M. Wang, and K. J. Stebe, Proc. Natl. Acad. Sci. U.S.A. **108**, 20923 (2011).
[28] L. Botto, E. P. Lewandowski, M. Cavallaro, and K. J. Stebe, Soft Matter **8**, 9957 (2012).
[29] C. Zeng, F. Brau, B. Davidovitch, and A. D. Dinsmore, Soft Matter **8**, 8582 (2012).
[30] A. He, K. Nguyen, and S. Mandre, Europhys. Lett. **102**, 38001 (2013).
[31] C. Camoin, J. Roussell, R. Faure, and R. Blanc, Europhys. Lett. **3**, 449 (1987).
[32] O. D. Velev, N. D. Denkov, V. N. Paunov, P. A. Kralchevsky, and K. Nagayama, Langmuir **9**, 3702 (1993).
[33] C. D. Dushkin, P. A. Kralchevsky, H. Yoshimura, and K. Nagayama, Phys. Rev. Lett. **75**, 3454 (1995).
[34] C. D. Dushkin, P. A. Kralchevsky, V. N. Paunov, H. Yoshimura, and K. Nagayama, Langmuir **12**, 641 (1996).
[35] C. D. Dushkin, H. Yoshimura, and K. Nagayama, J. Colloid Interface Sci. **181**, 657 (1996).
[36] J. M. Rieser, P. Arratia, A. Yodh, J. P. Gollub, and D. Durian, Langmuir **31**, 2421 (2015).

[37] N. D. Vassileva, D. van den Ende, F. Mugele, and J. Mellema, Langmuir **21**, 11190 (2005).
[38] M.-J. Dalbe, D. Cosic, M. Berhanu, and A. Kudrolli, Phys. Rev. E **83**, 051403 (2011).
[39] R. Di Leonardo, F. Saglimbeni, and G. Ruocco, Phys. Rev. Lett. **100**, 106103 (2008).
[40] B. J. Park and E. M. Furst, Soft Matter **7**, 7676 (2011).
[41] V. Carrasco-Fadanelli and R. Castillo, Soft Matter **15**, 5815 (2019).
[42] E. Mansfield, H. Sepangi, and E. Eastwood, Phil. Trans. R. Soc. A **355**, 869 (1997).
[43] J. B. Keller, Phys. Fluids **10**, 3009 (1998).
[44] D. Vella, Annu. Rev. Fluid Mech. **47**, 115 (2015).
[45] D. Jiles, *Introduction to Magnetism and Magnetic Materials* (CRC Press, Boca Raton, 2015).
[46] See Supplemental Material at http://link.aps.org/supplemental/10.1103/PhysRevLett.123.254502 for extended details on experimental methods, error analysis, video of typical experimental run, and numerical methods.
[47] P.-G. de Gennes, F. Brochard-Wyart, and D. Quéré, *Capillarity and Wetting Phenomena: Drops, Bubbles, Pearls, Waves* (Springer Science & Business Media, New York, 2013).
[48] J. W. Bush and D. L. Hu, Annu. Rev. Fluid Mech. **38**, 339 (2006).
[49] J.-S. Koh, E. Yang, G.-P. Jung, S.-P. Jung, J. H. Son, S.-I. Lee, P. G. Jablonski, R. J. Wood, H.-Y. Kim, and K.-J. Cho, Science **349**, 517 (2015).
[50] Y. Chen, H. Wang, E. F. Helbling, N. T. Jafferis, R. Zufferey, A. Ong, K. Ma, N. Gravish, P. Chirarattananon, M. Kovac *et al.*, Sci. Robot. **2**, 5619 (2017).
[51] Y. Chen, N. Doshi, B. Goldberg, H. Wang, and R. J. Wood, Nat. Commun. **9**, 2495 (2018).
[52] R. Chinomona, J. Lajeunesse, W. H. Mitchell, Y. Yao, and S. E. Spagnolie, Soft Matter **11**, 1828 (2015).
[53] G. Grosjean, G. Lagubeau, A. Darras, M. Hubert, G. Lumay, and N. Vandewalle, Sci. Rep. **5**, 16035 (2015).
[54] G. Pucci, I. Ho, and D. M. Harris, Sci. Rep. **9**, 4095 (2019).
[55] B. Madivala, S. Vandebril, J. Fransaer, and J. Vermant, Soft Matter **5**, 1717 (2009).
[56] E. P. Lewandowski, J. A. Bernate, A. Tseng, P. C. Searson, and K. J. Stebe, Soft Matter **5**, 886 (2009).
[57] G. Soligno, M. Dijkstra, and R. van Roij, Phys. Rev. Lett. **116**, 258001 (2016).
[58] A. Würger, Phys. Rev. E **74**, 041402 (2006).
[59] J. Guzowski, M. Tasinkevych, and S. Dietrich, Phys. Rev. E **84**, 031401 (2011).
[60] C. Blanc, D. Fedorenko, M. Gross, M. In, M. Abkarian, M. A. Gharbi, J.-B. Fournier, P. Galatola, and M. Nobili, Phys. Rev. Lett. **111**, 058302 (2013).
[61] P. Galatola and J.-B. Fournier, Soft Matter **10**, 2197 (2014).
[62] A. A. Evans, S. E. Spagnolie, D. Bartolo, and E. Lauga, Soft Matter **9**, 1711 (2013).
[63] G. Falkovich, A. Weinberg, P. Denissenko, and S. Lukaschuk, Nature (London) **435**, 1045 (2005).
[64] M. De Corato and V. Garbin, J. Fluid Mech. **847**, 71 (2018).
[65] A. Huerre, M. De Corato, and V. Garbin, Nat. Commun. **9**, 3620 (2018).
[66] A. Domínguez, M. Oettel, and S. Dietrich, Phys. Rev. E **82**, 011402 (2010).
[67] J. Bleibel, S. Dietrich, A. Domínguez, and M. Oettel, Phys. Rev. Lett. **107**, 128302 (2011).
[68] J. Bleibel, A. Domínguez, M. Oettel, and S. Dietrich, Eur. Phys. J. E **34**, 125 (2011).
[69] S. Karpitschka, A. Pandey, L. A. Lubbers, J. H. Weijs, L. Botto, S. Das, B. Andreotti, and J. H. Snoeijer, Proc. Natl. Acad. Sci. U.S.A. **113**, 7403 (2016).